Atmos. Chem. Phys. Discuss., 11, 22129–22172, 2011
www.atmos-chem-phys-discuss.net/11/22129/2011/
doi:10.5194/acpd-11-22129-2011

Atmospheric Chemistry and Physics Discussions

Extension of an assessment model of ship traffic exhaust emissions for particulate matter and carbon monoxide

J.-P. Jalkanen[1], L. Johansson[1], J. Kukkonen[1], A. Brink[2], J. Kalli[3], and T. Stipa[1]

[1]Finnish Meteorological Institute, P.O. Box 503, 00101 Helsinki, Finland
[2]Åbo Akademi, Process Chemistry Center (CMC), Tuomiokirkontori 3, 20500 Turku, Finland
[3]University of Turku, Centre for Maritime Studies, P.O. Box 181, 28101 Pori, Finland

Received: 9 June 2011 – Accepted: 11 July 2011 – Published: 5 August 2011

Correspondence to: J.-P. Jalkanen (jukka-pekka.jalkanen@fmi.fi)

Published by Copernicus Publications on behalf of the European Geosciences Union.

Abstract

A method is presented for the evaluation of the exhaust emissions of marine traffic, based on the messages provided by the Automatic Identification System (AIS), which enable the positioning of ship emissions with a high spatial resolution (typically a few metres). The model also takes into account the detailed technical data of each individual vessel. The previously developed model was applicable for evaluating the emissions of NO_x, SO_x and CO_2. This paper addresses a substantial extension of the modelling system, to allow also for the mass-based emissions of particulate matter (PM) and carbon monoxide (CO). The presented Ship Traffic Emissions Assessment Model (STEAM2) allows for the influences of accurate travel routes and ship speed, engine load, fuel sulphur content, multiengine setups, abatement methods and waves. We address in particular the modeling of the influence on the emissions of both engine load and the sulphur content of the fuel. The presented methodology can be used to evaluate the total PM emissions, and those of organic carbon, elemental carbon, ash and hydrated sulphate. We have evaluated the performance of the extended model against available experimental data on engine power, fuel consumption and the composition-resolved emissions of PM. As example results, the geographical distributions of the emissions of PM and CO are presented for the marine regions surrounding the Danish Straits.

1 Introduction

Currently available global ship emission inventories for particulate matter (PM) are mostly based on from top to down (i.e. top-down)-approaches. However, the statistics concerning the sales of marine fuels are difficult to disaggregate to the amounts of fuel burned regionally or locally. The approaches based on fleet activities, called as bottom-up methods, have therefore recently gained popularity; new ship emission inventories have been generated especially for arctic regions (Paxian et al., 2010; Corbett et al., 2010). Various regional ship emission inventories have been introduced (Matthias et al., 2010; De Meyer et al., 2008) and the previously significant uncertainties in the estimated emissions of global ship traffic have been evaluated to have decreased during the last half decade (Paxian et al., 2010; Lack et al., 2008).

Information is currently scarce especially regarding the geographical distribution and chemical composition of PM emissions arising from ship traffic, and the chemical composition details have not commonly been introduced to global bottom-up inventories of ship emissions. However, Corbett et al. (2010) subdivided PM from marine traffic into organic carbon and black carbon. They did not allow for the dependency on engine load of the constituents of PM; instead, fixed, predetermined loads were used for main and auxiliary engines. Inclusion of arctic areas in ship emission inventories without allowing for the effects of sea ice on ship performance can lead to significant uncertainties in the predicted emissions.

There are several situations, in which decreasing the speed of a vessel or maneuvering in port areas will result in changes of the engine loads and chemical composition of PM emissions; examples of such conditions are slow steaming and ships that are breaking ice cover (Winnes and Fridell, 2010a). In such conditions, the assumptions of pre-determined engine loads and static emission factors are not valid. In case of slow steaming, the effects of running the engines of ships on abnormally low loads result in increased emissions in most marine diesel engines. However, this is not necessarily the case for multi-engine setups or combined diesel-electric installations, since unnecessary engines can be switched off to conserve fuel and taken to operation whenever needed. The influences of such more detailed features involving engine operation and engine load, including multi-engine setups, are practically neglected in all currently available ship emissions inventories.

The authors of this article have previously presented a method for the evaluation of the exhaust emissions of marine traffic, based on the messages provided by the Automatic Identification System (AIS), which enable the identification and location determination of ships (Jalkanen et al., 2009). The use of the AIS data facilitates the

Discussion Paper | Discussion Paper | Discussion Paper | Discussion Paper |
ACPD
11, 22129–22172, 2011
An assessment model of ship traffic exhaust emissions
J.-P. Jalkanen et al.

positioning of ship emissions with a high spatial resolution, which is limited only by the inaccuracies of the Global Positioning System (typically a few meters). The previously developed model was applicable for evaluating the emissions of NO_x, SO_x and CO_2. The model was based on the relationship of the instantaneous speed to the design speed and the use of the detailed technical information of the engines. The effect of waves was also included in the model. However, the methodologies for evaluating the power and fuel consumption were fairly simple, and these assumptions were observed to provide biased estimates, especially for auxiliary engines.

There have previously been major uncertainties in assessing the emissions from ship traffic, caused by the uncertainties of evaluating the times of ships spent at sea and at berth. However, using the AIS data almost totally removes these uncertainties. The instantaneous speeds of the vessels are also known from the AIS data, the use of which substantially reduces the uncertainties in analyzing the operational states of the ship engines. International ship emissions are not part of the routine reporting under the Convention on the Long-Range Transport of Atmospheric Pollutants (CLRTAP); the improvement of the description of emissions from the maritime transport sector (European Environment Agency, 2009) is laborious because a large part of the work requires significant manual contribution.

Using the STEAM model, engine loads during voyages can be determined with reasonable accuracy based on the ratio of ship speed and the calculated resistance that the ship is required to overcome at a specified speed. This can be done even for ships with multi-engine setups. To our understanding these features have not currently been included in the existing global inventories of Corbett et al. (2010) and Paxian et al. (2010). Both of the models used in computing the above-mentioned two inventories are well suited for evaluating future scenarios. On the other hand, the measured AIS data offers highly detailed information of the past and present state of maritime traffic. Clearly, the use of AIS data eliminates the need to computationally construct the ship routes.

ACPD
11, 22129–22172, 2011

In contrast to top-down emission inventories, generated based on the fuel sales or cargo statistics (Schrooten et al., 2009), within the STEAM model, the port emissions are included by default. These emissions have previously been neglected in many studies, due to their complexity regarding engine operating modes and different fuel types (Hulskotte and Denier van der Gon, 2010; Cooper, 2003). Evaluation of shipping emissions in port areas is challenging, caused by the dependency of emissions on engine load, the changes of fuel type and the differences of operating profiles of ships at berth, during maneuvering and during normal cruising.

However, the emissions of both the various chemical components of PM and CO are highly sensitive on engine load. The classifications of PM components, and the detailed definitions of such classes also can vary, depending on the experimental techniques used. For instance, the experimental methods using absorptive techniques often provide black carbon (Eyring et al., 2010), but chemical techniques report a division to elemental and organic carbon. Clearly, black carbon and elemental carbon cannot be used as synonymous expressions, since there are components of organic carbon, which also absorb light (Andreae and Gelencsér, 2006).

Emissions of PM from shipping have a significant impact on ambient air quality in densely populated coastal areas and these may substantially contribute to detrimental impacts on human health (Corbett et al., 2007). Stringent limits for the sulphur content of marine fuels and NO_x-emissions are expected to reduce the emissions from ships. The PM emissions are simultaneously reduced, as a major part of PM emissions is in the form of sulphate. However, sulphur content reductions will not eradicate PM emissions completely (Winnes and Fridell, 2010b; Fridell et al., 2008; Cooper, 2003, 2006; Kasper et al., 2007; Buhaug et al., 2009), even if the global fleet would switch to low sulphur fuel. The emissions of PM can also be reduced by using after-treatment techniques, which will remove a significant part of the PM emissions (Corbett et al., 2010; European Commission Directorate General Environment, 2005). Scrubbing systems from engine manufacturers have been commonly applied to diesel power plants on land, but their commercial installations to ships have been scarce. This is expected to change, after the implementation of the stringent sulphur limits included in the revised Marpol Annex VI of the IMO (International Maritime Organization, 1998).

This paper describes a refined STEAM model, called in the following STEAM2. We have developed a more sophisticated scheme for the resistance evaluation and a load balancing of the engines; these improvements were necessary especially for the accurate modeling of PM and CO emissions. The STEAM2 model is also more versatile compared with the original model in describing the effects of ship speed and movement, engine load and fuel changes, abatement techniques, and operating profiles of vessels. The methods to model the effect of waves to ship emissions are identical to those in the earlier version of the model (Jalkanen et al., 2009). The earlier version of the STEAM model already included the various effects of emission abatement techniques. These are also included in the STEAM2 model and applied to the evaluation of the emissions of PM and CO whenever appropriate. However, the number of vessels with abatement techniques installed is less than 1 % of all the vessels in the ship properties database.

The information on each individual ship and the installed main and auxiliary engines were obtained from IHS Fairplay (IHS Fairplay, 2010), but augmented with data from various other sources (such as other classification societies and ship owners), whenever necessary. This concerns in particular fuel types and abatement techniques. Modeled fuel consumption or emissions can be directly compared with monthly or annual fuel reports of the ship owners, or with the emission measurements to evaluate the model performance.

The objectives of this article are (i) to present the principles and mathematical structure of the extended ship emission model (STEAM2), (ii) to compare the predictions of the extended model with those of the original model (STEAM), regarding the instantaneous power and fuel consumption, using onboard engine measurements, (iii) to evaluate the extended model against available experimental data, and (iv) to illustrate the capabilities of the model by presenting some selected numerical results. Emission estimates provided by the model have been compared to the available measurements

ACPD
11, 22129–22172, 2011

presented in recent literature. As examples, the geographical distributions of the emissions of PM and CO are presented for the southern regions of the Baltic Sea. The computational system presented in this study could be extended to be global, as soon as a global coverage of satellite-AIS would be available.

2 The STEAM2 model

An illustration of the main components of the STEAM2 model is presented in Fig. 1. The main input data sources are the internal ship database (compiled in this study) and the AIS-data.

The internal ship database of the STEAM2 model contains the technical details of ships used in the evaluation of emissions. The database contains the information of more than 30 000 ships; this is approximately a third of the global fleet. Most of the ships in the database are newer ships that have been built within the last two decades; most of these ships are frequently operating in the Baltic Sea.

The use of the AIS data facilitates an accurate mapping of the ship traffic, including the detailed instantaneous location and speed of each vessel in the considered area. For example, more than 210 million so-called position reports were received from the 9497 AIS targets in the Baltic Sea in 2007. The automatic position reports contain the detailed information on the identification, location, speed and heading of each individual vessel. For each ship in a regular schedule, this results in tens of thousands of position updates each month.

Based on the properties of the ships and its power requirements, the model can evaluate the power consumption and load of the engine, and the fuel consumption of the ship. Based on these values, the model is used to evaluate the emissions of NO_x, SO_x, CO, CO_2 and PM, as a function of time and location.

The main differences between the new model (STEAM2) and the previously developed one (STEAM) include that the CO- and PM emissions are included in the latter model. A new evaluation method is also used for analyzing the resistance of ships

ACPD
11, 22129–22172, 2011

in water. The mode also includes a refined modeling of the power consumption of auxiliary engines, which depend on ship type and its operation mode.

2.1 The evaluation of resistance and ship specifications

A method presented by Hollenbach (1998) is used to calculate the resistance of ships due to moving in water. The predictions of the Hollenbach method agree well with other performance prediction methods, such as those of Holtrop-Mennen (Matulja and Dejhalla, 2007; Holtrop and Mennen, 1982; Holtrop and Mennen, 1978). The use of this method, compared with the previous model, improves the predictions of resistance and engine power, especially in cases, in which the hull dimensions and the engine data is available, but the design speed of the vessel is unknown. In the previous version of the STEAM model, the design speed was a critical parameter for the model performance; if that value was not available, an average speed was used instead that was specific for each ship type. The use of the Hollenbach method avoids such assumptions, and therefore provides a more reliable basis for the resistance calculations.

The Hollenbach method is based on the resistance measurements in 433 tank tests. However, the application of the method is in many cases limited by the availability of the hull and propeller details. To overcome this difficulty, a way of estimating the Block coefficient was used, as suggested by Watson and Gilfillan (1976) and further described by Townsin (1979). The Block coefficient is one of the coefficients describing the shape of the hull and it can be written as

$$C_\mathrm{b} = 0.7 + \frac{1}{8} atan\left(\frac{23 - 100F_n}{4}\right) \tag{1}$$

where F_n is Froude number, which is computed as speed/(gravity constant * waterline length). Neither waterline length nor the length over surface (used by the Hollenbach method) was readily available for most of the vessels. In these cases, we used instead an average value of overall length in meters (LOA) and length between perpendiculars in meters (LBP).

ACPD
11, 22129–22172, 2011
An assessment model of ship traffic exhaust emissions
J.-P. Jalkanen et al.

For reliable power predictions using this model, either propeller revolutions per minute (rpm) or propeller size has to be known. Propeller rpm is required to estimate the propeller and transmission losses and the required main engine power. If the number of propellers is unknown, then the ship is simply assumed to operate with a single propeller. Propeller diameter is estimated using the method described by Watson (1998). An estimate for the propeller diameter d in meters is

$$d = 16.2 \frac{P_s^{0.2}}{N^{0.6}} \quad (2)$$

where P_s is the service power of the main engine (80 % of the maximum continuous rating) provided by IHS Fairplay (2010) in kilowatts and N is the propeller's rpm. This method was used for all single-propeller vessels, for which the propeller rpm was known. For multi-propeller vessels, if both the propeller rpm and diameter were unknown, a value was used that is based on a fraction of vessel draught. This approach does not consider exceptional cases of surface piercing propellers. It is expected to lead to a reasonable estimate of propeller diameter. In multi-propeller cases and also if propeller data is unavailable, propeller size is estimated with a ship type specific fraction of draught, as draught is one of the main limiting factors for propeller size. Fractions of draught values, which have been estimated using the internal ship database, are listed in Appendix A.

The number of bossings (hubs) is assumed to be equal to the number of propellers, and the number of thrusters and rudders were fixed to one, and the number of propeller shafts was set to match the number of propellers. Thruster information is in many cases not included in the technical details; however, the contribution of thrusters to overall wet surface area is small. If propeller rpm was not specifically known, it was estimated based on Eq. (2).

The main engine power can never be completely transformed to actual propelling power of the ship. The dimensionless quasi propulsive constant η_d is used to describe the effectiveness of converting the main engine power to actual propelling power, taking

ACPD
11, 22129–22172, 2011
An assessment model of ship traffic exhaust emissions
J.-P. Jalkanen et al.

propulsive losses arising from transmission, hull, shaft and propeller itself into account. According to Watson (1998) it can be written as

$$\eta_d = 0.84 - \frac{N\sqrt{\mathrm{LBP}}}{10\,000} \tag{3}$$

where N is the rpm of the propeller and LBP is the length between perpendiculars. Propeller efficiency is commonly substantially less than unity; usually 60–80 % of the main engine power is transmitted to the water by the propeller (Watson, 1998). If propeller rpm cannot be determined from ship technical data and it cannot be estimated using Eqs. (2) and (3), the power is predicted based on the previous version of the model (Jalkanen et al., 2009). In these cases, 80 % of the main engine power is assumed to be in use, when the vessel is traveling at its design speed. The required power is computed applying a relationship kv^3, where k is a ship-specific constant generated from main particulars and v is the instantaneous speed of the vessel.

In the internal ship database sufficient propeller details exist for about 60 % of the cases, which facilitate the evaluation of the quasi propulsive constant. In the remaining cases, the previous method (Jalkanen et al., 2009) of engine power estimation for the main engines has to be used, which requires that the design speed of the ship has to be known. In approximately five percent of the ship database entries both the propeller rpm and vessel design speed are missing. In such cases, the emission predictions are relatively less accurate, as average values specific to this ship type have to be used as a substitute for the missing ship data values. The values larger than the total installed engine power are not allowed for by the model.

2.2 Operating characteristic of engines

In addition to the prediction of the instantaneous main engine power also auxiliary engine power is needed to describe the total exhaust emissions. Furthermore, variable engine loads will have a significant impact on fuel consumption and emissions of CO and PM. Each of these features will be discussed in consecutive chapters, starting from load determination and its impact on fuel consumption.

ACPD
11, 22129–22172, 2011

2.2.1 The load balancing for multi-engine installations

A load balancing scheme for multi-engine installations has also been implemented in the STEAM2 model. Load balancing is a crucial issue for the proper functioning of multi-engine installations. Engines that are not needed at a specific moment can be turned off, which saves fuel and ensures that the remaining engines are operated with an optimal engine load. To simulate this operation of the engines, the STEAM2 model determines the minimum number of engines, which need to be in operation to overcome the predicted resistance of the ship.

Clearly, the engine load, i.e. ratio of currently used power and installed power, affects fuel consumption and the emissions of PM and CO. While it is straightforward to estimate an engine load of a single engine ship, if required power is known, this estimation is more challenging for multi-engine setups. The model estimates the engine power needed to achieve the ship speed as reported in the AIS position reports, using a resistance calculation by the Hollenbach method. Total instantaneous engine power is compared against the capabilities of each engine.

The model assumes all main engines to be identical, a minimum number of engines are assumed to be used, and the load values are assumed to be less or equal than 85 %. The latter assumption is needed, as engine loads larger than 85 % are commonly avoided. If this load value would be exceeded, an additional engine is assumed to be taken online and the load is balanced among the operational engines. For example, let us consider a ship with four installed engines, each with a power of 6 MW, and an instantaneous power requirement of 11 MW. The minimum requirement to obtain 11 MW would require operation of two engines at 91.7 % load level, which is not feasible. The modeling assumption is therefore that three engines would be used instead, each with a load of 61.1 %.

A limitation of this approach is that the model treats all main engines as equal and neglects engine setups, for which one engine in a pair is larger than another. For instance, in case of four engines with two pairs of identical engines, a so-called 2 + 2

ACPD
11, 22129–22172, 2011

setup, the accuracy of the predictions of fuel consumption and emissions will deteriorate. Passenger classed vessels and ships with more than one propeller are required to have at least two engines operational at all times due vessel safety rules. Load balancing is applied to both main and auxiliary engines, but in case of diesel-electric engine setups, all the power commonly required for ship systems and propulsion is taken from the main engines. In such cases, the main engines are operated to generate electricity, and electrical motors are used as propulsion. Diesel engines do not run the ship directly in these cases and no auxiliary engines are used.

2.2.2 The evaluation of auxiliary power

The previous model estimated auxiliary power using ship type classification and three different operation modes for the ship. In STEAM2, auxiliary engine usage is evaluated as in previous model, but with the following modifications: Passenger class vessels (cruise ships, RoRo/passenger and yacht) use a base value of 750 kW of auxiliary engine power for all operating modes, but an additional requirement of 3 kW is added for each cabin. This emulates the additional need for electricity required by air conditioning, hot water and other electrical installations inside the cabins. For reefers and containerships, similar assumptions are applied. A base value of 750 kW is used while cruising, 1000 kW during hoteling and 1250 kW while maneuvering. In addition to these values, each refrigerated Twenty-foot Equivalent Unit (TEU, standardized cargo container) consumes approximately 4 kW of electricity to maintain the containers in a constant temperature. Clearly, the actual power requirement of the container depends on the temperature difference between the environment and the container (Wild, 2009).

All other vessel classes use 750, 1000 and 1250 kW for cruising, hoteling and maneuvering, respectively. With these modifications, STEAM2 can distinguish between large and small vessels of the same ship type. However, in all cases, the installed auxiliary engine power is used as an upper limit for the predicted auxiliary engine power (in cases, for which the computed auxiliary power would exceed the installed auxiliary power). Boiler energy usage is included in the estimates of auxiliary engine power; these have not been modeled explicitly due to the lack of data.

ACPD
11, 22129–22172, 2011

2.2.3 The impact of engine load on specific fuel oil consumption

Instantaneous total fuel consumption is influenced by many independent factors. Fuel consumption of main engines used in propulsion is commonly estimated in available literature as a product of the constant specific fuel oil consumption (SFOC) and instantaneous engine power, which results in a linear relationship between fuel consumption and engine power. Ideally, all power systems that require fuel to operate should be modeled separately, such as the main engines for propulsion, the auxiliary engines for power generation and the boilers for heat generation. However, in practice a separate modeling of all of these is currently not feasible.

The relative SFOC curve provided by the engine manufacturer Wärtsilä for a medium sized 4-stroke engine is presented in Fig. 2. Using SFOC-studies and engine specifications (Caterpillar, 2010; Man B&W, 2010), two other relative SFOC-curves by other manufacturers are also presented. The engines by MAN considered here are large 2-stroke models, whereas the Caterpillar engines are relatively small 4-stroke models.

For all three curves presented, the SFOC is a non-linear function of engine load, and this function has a minimum at a specific engine load. For the data of Caterpillar, MAN and Wärtsilä, the minimum is approximately at the relative engine load of 70, 75 and 80 %, respectively. Minimizing fuel oil consumption therefore requires engine loads approximately from 70 to 80 % which represents the optimum regime in terms of both consumption and performance. There is an approximately parabolic dependency between the SFOC and the engine load.

In the STEAM2 model, we have assumed a parabolic function for all engines. Using regression analysis of the comprehensive SFOC-measurement data from Wärtsilä, we derived a second degree polynomial equation for the relative SFOC:

$$\mathrm{SFOC}_{\mathrm{Relative}}(EL) = 0.455\mathrm{EL}^2 - 0.71\mathrm{EL} = 1.28 \quad (4)$$

where EL is the engine load ranging from 0 to 1. The absolute fuel consumption is estimated from

$$\mathrm{SFOC(EL)} - \mathrm{SFOC}_{\mathrm{Relative}}(\mathrm{EL}) \cdot \mathrm{SFOC}_{\mathrm{base}} \quad (5)$$

where $SFOC_{base}$ is the so-called base value for SFOC that is a constant for each engine. According to second IMO greenhouse gas report (Buhaug et al., 2009), a lower consumption is assigned for new engines, describing the technical development and better efficiency of modern engines. The base value is also influenced by engine stroke type and power. We use primarily engine-model specific base values of SFOC from the engine manufacturers. If such a value is not available, the value is evaluated (taking the above mentioned factors into account) according to the IMO GHG2 report (Buhaug et al., 2009).

For simplicity, it has been assumed that engine load and SFOC –dependence from Eqs. (4) and (5) applies to all engines. For turbine machinery, $SFOC_{base}$ of 260 g kWh^{-1} is used. Auxiliary engine $SFOC_{base}$ was set to 220 g kWh^{-1} and the same load dependency was applied. In case of diesel-electric engine setups, the power normally generated using auxiliary engines was added to main engine power and engine loads were determined accordingly. However, diesel engines with common rail fuel injection technology may show a different behavior compared to the one described above. This should be taken into account in the future, as the fraction of common rail diesel engines is expected to increase.

2.3 The exhaust emissions

In STEAM2, PM is divided into Elementary Carbon (EC), Organic Carbon (OC), Ash, Sulphate (SO_4) and associated water (H_2O). The carbon monoxide (CO) emissions are also modelled. Clearly, the main aim is that the model would provide accurate emission factors for the all pollutants, including all the chemical components of PM, for all values of the fuel sulphur content throughout whole operating load range. The evaluation of the influence of engine load is needed especially for an accurate description of emissions of PM, CO and CO_2. All emissions have therefore been assumed to be dependent on engine load, except for those of NO_x, which are only slightly dependent.

Emissions of particulate matter and SO_x depend on the fuel consumption of the ship, whereas emissions of NO_x mainly depend on the temperature and the duration of the

ACPD

11, 22129–22172, 2011

An assessment model of ship traffic exhaust emissions

J.-P. Jalkanen et al.

combustion cycle. Emissions of carbon monoxide depend not only on engine load and engine power, but also on the gradient of engine power. Acceleration of ship results in incomplete combustion of fuel and relatively higher emissions of CO. As discussed previously, fuel consumption is dependent on engine load; the emissions of several pollutants have the same dependency. Several authors have reported experimental results on the composition of particulate matter as a function of engine load (Agrawal et al., 2008, 2010; Petzold et al., 2008; Moldanová et al., 2009; Sarvi et al., 2008a) and sulphur content (Sarvi et al., 2008b; Buhaug et al., 2009). These datasets represent cases where measurements over the whole load range with several types of fuel with variable sulphur content were available.

Additionally, load balancing facilitates the estimation of effectiveness of slow steaming. In these cases the ship decreases its speed to save fuel. However, if the engine is run outside its normal operating load range, emissions and fuel consumption will increase, since the engines are not commonly optimized to run on low loads for prolonged periods. This is correct for single engine installations, but for multi-engine installations, unnecessary engines can be turned off. This effect is taken into account by the model.

2.3.1 The emissions of PM in terms of fuel sulphur content and engine load

The sulphur content of the fuel has a crucial influence on the PM emissions. The dependency of PM emission factor on fuel sulphur content was modelled according to Buhaug et al. (2009), as presented in Fig. 3. As expected, the emission factors of the total PM, SO_4 and associated H_2O (i.e. H_2O chemically attached to sulphate) are linearly dependent on the fuel sulphur content, whereas the emission factors of EC and ash are almost independent of this factor. The emissions of PM could therefore not be eradicated totally, even if sulphur would be completely eliminated from ship fuels (Winnes and Fridell, 2010b; Buhaug et al., 2009). The measured total mass of particulate matter as defined here includes also the associated H_2O; the amount of which may substantially vary according to the experimental set-up and conditions during the exhaust measurements.

ACPD
11, 22129–22172, 2011

Applying linear regression analysis to the data presented in Fig. 3 yields the following emission factor dependencies:

$$EF_{SO_4}(S) = 0.312\, S \qquad (6a)$$

$$EF_{H_2O}(S) = 0.244\, S \qquad (6b)$$

and

$$OC(\text{load}) \begin{cases} 3.333, \text{load} < 0.15 \\ \dfrac{A}{1 + B \cdot \exp(-C \cdot \text{load})}, \text{load} \geq 0.15 \end{cases} \qquad (6c)$$

$$EF_{EC} = 0.08 \frac{\text{g}}{\text{kWh}}, \; EF_{OC} = 0.2 \frac{\text{g}}{\text{kWh}}, \; EF_{Ash} = 0.06 \frac{\text{g}}{\text{kWh}} \qquad (6d)$$

where S is the fuel sulphur content in percentages and the emission coefficients for EC, OC and ash have been assumed to be independent of the sulphur content, but for OC an additional dependency on engine load is used. In Eq. (6c), the dimensionless constants are $A = 1.024$, $B = -47.660$, $C = 32.547$, respectively. The amount of ash may change between different fuel grades, but this effect is neglected for now. The total PM emission factor (in g kWh^{-1}) is assumed to be the following:

$$EF_{PM}(\text{load}, S) = SFOC_{\text{relative}}(\text{load}) \cdot [(0.312 + 0.244) S + OC(\text{load}) \cdot EF_{OC} + 0.14] \qquad (7)$$

In STEAM2, the PM emissions [g kWh^{-1}] are evaluated as the product of specific fuel-oil consumption and emission factors, where the relative SFOC is computed using Eq. (4). The variations of this emission factor have been graphically illustrated in Fig. 4.

The emissions of the chemical components of PM have been reported to change as a function of engine load (Agrawal et al., 2008a, b, 2010); this has been taken into account in the modeling of STEAM2. In STEAM2, the variation of the PM emission factor for different components has been modeled based on the variation of SFOC.

ACPD
11, 22129–22172, 2011
An assessment model of ship traffic exhaust emissions
J.-P. Jalkanen et al.

An additional dependency for OC is used as given in Eq. (6c) for which results from Agrawal et al. (2008a, b, 2010), Petzold et al. (2010) and Sarvi et al. (2008a) were used and fitted to a mathematical form. The emissions of all PM components are modeled based on the variations of SFOC and instantaneous power, and in addition the emission factors of sulphate and associated water are dependent on the fuel sulphur content.

2.3.2 The emissions of carbon monoxide

Assuming perfect combustion conditions, the amount of emitted CO_2 can be estimated in a straightforward manner from the amount of fuel burned. However, the CO emissions are substantially dependent on engine load. The data based on three experimental studies and the modeled dependency of the base emission factor of CO as a function of engine load has been presented in Fig. 5. The CO base emission factor as described by Sarvi (2008a) has been adopted in STEAM2, as it is based on a systematic inclusion of a wide range of engine loads.

During normal engine operation, when engine load ranges from 75 % to full load, the base emission factor of CO is small according to Sarvi (2008a). However, using the engine at low engine loads will significantly increase the CO emission factor.

A rapid change of engine load has been observed (Cooper, 2001, 2003) to result in increased emissions of carbon monoxide. This is usually the case, when the ship is accelerating or actively decelerating (braking). We have therefore modified the modeled curve (as presented above) with an additional scaling term, that amplifies the CO emission factor, if the ship is accelerating.

Using this scaling factor called Acceleration Based Component (ABC), the CO emissions takes the following form:

$$EF_{CO} = CO_{base} \cdot ABC \qquad (8)$$

where

ACPD
11, 22129–22172, 2011
An assessment model of ship traffic exhaust emissions
J.-P. Jalkanen et al.

$$ABC = \max\left\{\alpha\frac{|\Delta \mathrm{speed}|}{\Delta \mathrm{time}}, 1\right\} \quad (9)$$

For simplicity, the dimensionless empirical factor α has been assumed to be the same for all ships, $\alpha = 300$. Ship speed and time changes are knots and seconds, respectively. The ABC is 1.0, if there is no significant acceleration; otherwise it is larger than unity.

Strictly speaking the ABC value is ship-dependent. The parameter α is certainly a function of the total mass of the vessel and very likely also a function of hull shape, but the determination of its exact form requires further study. More experimental data would be needed to model these relationships in more detail. The modelling above cannot distinguish between natural deceleration (engines stopped) and active braking (ship using its engines to decelerate). The CO emissions might therefore be overpredicted in case of natural deceleration.

3 Model evaluation and example numerical results

In this chapter, we (i) compare the predictions of the STEAM2 model with those of the original model, (ii) evaluate the extended model against available experimental data, and (iii) present selected numerical results.

3.1 Evaluation and inter-comparison of the predictions of STEAM and STEAM2 for engine power and fuel consumption

An example comparison between the predictions on main engine power of the two model versions is presented in Fig. 6. The engine power data has been collected in this study at the engine room of a large RoPax (Roll On – Roll Off cargo/Passenger) vessel using its own data logging systems. The presented voyage was done in an archipelago area near Stockholm, Sweden, and in the vicinity of this archipelago, in April 2008. We have used this specific dataset, as it was the only one available in the

Baltic sea region. Measured power profiles, such as the one presented in Fig. 6, are difficult to obtain, as only a limited number of vessels have internal equipment suitable to collect this data.

The basic statistical measures of this comparison are presented in Table 1. The predicted main engine powers of both models are in a fairly good agreement with the measured values STEAM2 slightly under-estimating the engine power. The predictions of the STEAM2 model are moderately better than those of STEAM in terms of the mean absolute error, and vice versa in terms of the mean error. There are physical factors that have been neglected in both models, such as the influences of the sea ice on the kinetic energy of the ship, the squat effect and the sea currents. Both models would therefore be expected to under-predict the required engine power in most cases, except in a case with calm sea with no ice and a strong sea current coming from the stern.

Largest differences between the two model versions are found in the beginning and near the end of the voyage; in the latter stage the original version of STEAM clearly over-predicts the engine power. The Hollenbach method used in STEAM2 results in a steeper power curve compared with the corresponding method in STEAM, i.e. a relatively lower resistance for low ship speeds and a higher one for high speeds. The most substantial differences between the two models in case of the presented data are therefore expected for low ship speeds. The reported and predicted fuel consumption of a RoPax ship in 2007 has been presented in Fig. 7a–b. The STEAM2 model predicts the total fuel consumption fairly accurately and slightly over-predicts the fuel consumption of auxiliary engines and boilers. The older model version substantially over-predicts the latter consumption. A similar comparison for five RoPax-ships is presented in Fig. 8. No substantial differences are found in the performance of the two model versions.

3.2 Evaluation of the modelling of load balancing in STEAM2

The STEAM2 model determines the number of engines, which need to be operated to overcome the predicted resistance of the ship, and the engine load of all running

ACPD
11, 22129–22172, 2011

engines. We have evaluated the performance of this sub-module, by using the data from the cruise presented above (cf. Fig. 6).

There were four identical main engines in the vessel considered. The observed and predicted engine loads during the test cruise are presented in Fig. 9a–d. The overall accuracy of predicted engine loads is fairly good or good for most of the time in the cases presented. However, there is some inaccuracy in the initial stages of the voyage, and for the fourth predicted engine (i.e. the one used only for very limited time periods).

3.3 Evaluation of the PM emission factors

The emission factor predictions by STEAM2 are compared with measurements available from literature in Fig. 10. The engines loads and fuel sulphur contents in these studies are as follows: 85 % and 2.85 % (Agrawal et al., 2008), 84 % and 1.90 % (Moldanova et al., 2009), 85 % and 2.21 % (Agrawal et al., 2008b), and 57 % and 3.01 % (Murphy et al., 2009). For simplicity, these studies are in the following referred to as AGR, MOL, PET and MUR. The engine load is within the commonly used operation range for the three first-mentioned studies, but it was substantially lower in MUR. The sulphur content of fuels varies from 1.9 to 3.0 %.

For a substantial fraction of these predictions, STEAM2 is in agreement with the measurements; the agreement is best in case of AGR. However, there are also significant differences. The most significant differences are found in comparison with the data by MOL, especially for OC and SO_4. The predicted sulphate emission factor is approximately three times larger than the measured value. According to MOL, the measured low sulphur conversion to sulphate may be a result of the relatively smaller amounts of V and Ni in the fuel, compared with, e.g. AGR. The catalytic properties of Ni and V enhance the sulphur conversion to sulphate.

According to Petzold et al. (2010), the conversion efficiency of fuel sulphur to particulate sulphate is linearly increasing with increasing engine load from 1 to 5 % (such a dependency is not allowed for in STEAM2). This could be one of the reasons for the deviations of predictions and data in case of MUR, due to the low engine load. A

ACPD
11, 22129–22172, 2011

detailed investigation of the complete data set of Petzold et al. (2010) using STEAM2 reveals an increasing difference in S to particulate SO_4 conversion with decreasing engine loads.

In case of MUR and AGR, the ash emission factor was computed from the ash content of the fuel, whereas MOL and PET report directly measured values of ash. These ash emission factors are therefore not directly comparable with each other, and the MUR and AGR ash emission values are strictly speaking not comparable with the STEAM2 predictions. There may be processes during fuel combustion, which lead to changes in the amount of emitted ash. MOL reports the highest ash emissions, although the ash content of the fuel used by MOL is the lowest. In comparison with PET, the STEAM2 ash emission factors are in a good agreement. The ash emissions in principle depend on the ash content of the fuel, but this is not taken into account in the model. However, one cannot conclude based on the above comparison of predictions and data that this would be a significant impact.

The water content of PM in these four datasets varies significantly. This can be due to differences in the experimental setups, sampling conditions and reporting. Water and organic compounds may condense on particulate surfaces after fuel combustion. Dilution and cooling of the PM sample to a lower concentration and temperature have an effect on the amount of condensed water. The amount of water is commonly calculated assuming a constant ratio of SO_4 and water (Agrawal et al., 2008a, b, 2010; Petzold et al., 2008). To overcome these difficulties, a dry PM mass could be used instead; however, this would require the inclusion of aerosol condensation processes. In STEAM2, the associated water is modelled separately (according to the IMO GHG2 study), and the user has an option to exclude it.

3.4 Predicted emissions of CO and PM in a selected marine area

The STEAM2 model can be used, e.g. for very detailed evaluations of the geographical and temporal distribution of marine emissions. As an example application of the model, a geographical distribution of CO and PM emissions from shipping has been presented in Figs. 11a–b in the marine regions surrounding the Danish Straits in January 2009. This region has been selected as an example, as it is the most densely trafficked region in the Baltic Sea.

Marine diesel engines commonly do not emit major amounts of CO during normal operation conditions; however, temporally variable engine loads can result in an incomplete combustion of fuel, and therefore significantly increase the emissions. This influence of emissions in the vicinity of major harbors is therefore clearly visible in Fig. 11a. The emissions of PM are focused in the vicinity of the most congested ship routes in this region and in harbor areas of Gothenburg (SWE), Copenhagen (DK), Kiel (GER), Lübeck (GER), Rostock (GER), Sassnitz (PL) and winoujcie/Szczecin (PL).

The currently available emission inventories have used emission factors that are not dependent on the changes of vessel speed and engine load. The detailed shipping inventories using the presented modeling system will therefore result in a substantially different geographical distribution of ship emissions, compared with the previous available ship emissions inventories.

4 Conclusions

The use of the AIS data facilitates an accurate mapping of the ship traffic, including the detailed instantaneous location and speed and of each vessel in the considered area. The presented model allows for the influences of a comprehensive range of relevant factors, including accurate travel routes and ship speed, engine load, fuel sulphur content, multiengine setups, abatement methods and waves. The presented model is the only method in the available literature that includes such a range of effects. Shipping routes and speed changes are included specifically and there is no need to guess which routes ships may take during the voyage.

The relatively largest uncertainties of the model predictions presented probably arise from the use of various types of fuel (Hulskotte and Denier van der Gon, 2010) but this is common to all ship emission inventories. It is challenging to extract the detailed data

ACPD
11, 22129–22172, 2011
An assessment model of ship traffic exhaust emissions
J.-P. Jalkanen et al.

regarding the fuel types used in ships in various geographical areas. However, if the data is available on the fuel type or the sulphur content on ship level, the model can dynamically adjust itself accordingly, and provide emissions, facilitating also various abatement strategies. The model presented in this paper allows direct comparisons of instantaneous exhaust emissions with experimental stack measurements of individual ships, which can be used to validate the predicted emissions.

Another challenge is the scarcity of detailed composition-resolved experimental data on PM emissions. The emissions of the chemical components of PM should be analyzed at various engine loads, and using various fuels, in order to be able to more comprehensively analyze and evaluate the performance of the modeling approaches. Further research is also needed to model various environmental effects, such as the influence of sea ice and marine currents; the former has a significant impact especially in the arctic and sub-arctic regions.

In previous emission inventories of marine traffic, constant load points and fixed emission factors have commonly been used and harbor emissions have been neglected. However, in order to obtain more accurate predictions, at least the dependence of shipping emissions on the location of the shipping routes, the actual speeds and engine loads have also to be taken into account. Changes of emission factors are especially important in port areas, as the European sulphur directive (EC/2005/33) states that the fuel used in EU harbor areas must not contain more than 0.1 % sulphur since the beginning of 2010. This directive will have a significant impact on the PM emissions from ships at berth, which should be taken into account by any model used in local scale modeling of harbor regions. There is an urgent need to reliably evaluate the effects of various policy options that focus on reducing the PM emissions from ships. The health and climatic influences can be substantially different for the various chemical constituents of PM; the modeling should therefore disaggregate the chemical fractions of PM emissions from ships.

The model presented can be extended for other marine regions besides the Baltic Sea, if the model input data will be available, including especially the AIS data.

ACPD
11, 22129–22172, 2011

However, the AIS data cannot be received across extensive sea areas, unless a satellite-based AIS reception is used. International cooperation between maritime authorities is therefore needed to be able to extend the model into a global scale.

Appendix A

The values of the fraction of draught for various ship types

The values of the fraction of draught are required in propeller size estimation for multi-propeller cases, and if propeller data is unavailable. The values, which are presented in Table A1, have been estimated in this study based on the ship database, using regression analysis.

Appendix B

Evaluation of the relative SFOC values against engine load

Relative SFOC curve used in the model is derived from the relative consumption values in Table B1 using regression analysis.

The engines of two other prominent marine engine manufactures, Caterpillar and MAN, have been studied in the same manner, although less thoroughly, using available information from engine specifications. Relative SFOC data was not available, but using the lowest SFOC value as the base value, the following data was acquired.

Acknowledgements. We gratefully acknowledge the support of the Finnish Transport Safety Agency (TraFi) and the member states of the Marine Environment Protection Committee of the Baltic Sea (Helcom) in this work. The research leading to these results has received funding from the European Regional Development Fund, Central Baltic INTERREG IV A Programme within the project SNOOP. The publication has been partly-produced in co-operation with the BSR InnoShip project (project no. #051 in the Grant Contract). The project is part-financed

ACPD
11, 22129–22172, 2011

by the EU Baltic Sea Region Programme 2007–2013, which supports transnational cooperation in the Baltic Sea region. The research leading to these results has also received funding from the European Union's Seventh Framework Programme FP/2007-2011 within the projects MEGAPOLI, grant agreement no. 212520, and TRANSPHORM, grant agreement no. 243406. This publication reflects the author's views and the Managing Authority of Central Baltic INTERREG IV A programme 2007–2013 cannot be held liable for the information published by project partners. This publication cannot be taken to reflect the views of the European Union.

References

Agrawal, H., Malloy, Q. G. J., Welch W. A., Miller, J. W., and Cocker III, D. R., Atmos. Environ., 42, 5504–5510, doi:10.1016/j.atmosenv.2008.02.053, 2008a.

Agrawal, H., Welch, W. A., Miller J. W., and Cocker, D. R.: Emission Measurements from a Crude Oil Tanker at Sea, Environ. Sci. Tech., 42, 7098–7103, doi:10.1021/es703102y, 2008b.

Andreae, M. O. and Gelencsér, A.: Black carbon or brown carbon? The nature of light-absorbing carbonaceous aerosols, Atmos. Chem. Phys., 6, 3131–3148, doi:10.5194/acp-6-3131-2006, 2006.

Buhaug, Ø., Corbett, J. J., Endresen, Ø., Eyring, V., Faber, J., Hanayama, S., Lee, D. S., Lee, D., Lindstad, H., Markowska, A. Z., Mjelde, A., Nelissen, D., Nilsen, J., Pålsson, C., Winebrake, J. J., Wu, W.-Q., and Yoshida, K.: Second IMO GHG study 2009; International Maritime Organization (IMO) London, UK, April 2009.

Caterpillar Inc.: Caterpillar 3208 Marine engine specification sheet, 1999.

Cooper, D. A.: Exhaust emissions from high-speed passenger ferries, Atmos. Environ., 35, 4189–4200, doi:10.1016/S1352-2310(01)00192-3, 2001.

Cooper, D. A.: Exhaust emissions from ships at berth, Atmos. Environ., 37, 4189–4200, doi:10.1016/S1352-2310(01)00192-3, 2003.

Corbett, J. J., Winebrake, J. J., Green, E. H., Kasibhatle, P., Eyring, V., and Lauer, A.: Mortality from ship emissions: a global Assessment, Environ. Sci. Technol., 41, 8512–8518, doi:10.1021/es071686z, 2007.

Corbett, J. J., Lack, D. A., Winebrake, J. J., Harder, S., Silberman, J. A., and Gold, M.: Arctic shipping emissions inventories and future scenarios, Atmos. Chem. Phys., 10, 9689–9704, doi:10.5194/acp-10-9689-2010, 2010.

De Meyer, P., Maes, F., and Volckaert, A.: Emissions from international shipping in the Belgian part of the North Sea and the Belgian seaports, Atmos. Environ., 42, 196–206, doi:10.1016/j.atmosenv.2007.06.059, 2008.

European Commission Directorate General Environment: Service contract on ship emissions: Assignment, Abatement and Market-Based Instruments, Task 2c, SO_2 abatement, ENTEC UK Ltd, 2005.

European Environment Agency: EMEP/EEA air pollutant emission inventory guidebook 2009, Technical guidance to prepare national emission inventories, EEA Copenhagen, 2009.

Eyring, V., Isaksenm, I. S. A., Berntsen, T., Collins, W. J., Corbett, J. J., Endresen, O., Grainger, R. G., Moldanova, J., Schlager, H., and Stevenson, D. S.: Transport impacts on atmosphere and climate: shipping, Atmos. Environ., 44, 4735–4771, doi:10.1016/j.atmosenv.2009.04.059, 2010

Fridell, E., Steen, E., and Peterson, K.: Primary particles in ship emissions, Atmos. Environ., 42, 1160–1168, doi:10.1016/j.atmosenv.2007.10.042, 2008.

Hollenbach, K. U.: Estimating resistance and propulsion for single-screw and twin screw ships, Ship Technology Research, 45/2, 1998

Holtrop, J. and Mennen, G. G.: A statistical power prediction method, International Shipbuilding Progress, 25, 253—256, 1978.

Holtrop, J. and Mennen G. G.: An approximate power prediction method, International Shipbuilding Progress, 7, 166–170, 1982.

Hulskotte, J. H. J. and Denier van der Gon, H.: Fuel consumption and associated emissions from seagoing ships at berth derived from an on-board survey, Atmos. Environ., 44, 1229–1236, doi:10.1016/j.atmosenv.2009.10.018, 2010.

IHS Fairplay: Lombard House, 3 Princess Way, Redhill, Surrey, RH1 1UP, UK, 2011.

International Maritime Organization (IMO): Regulations for the prevention of air pollution from ships and NO_x technical code, Annex VI of the MARPOL convention 73/78, London, 1998.

Jalkanen, J.-P., Brink, A., Kalli, J., Pettersson, H., Kukkonen, J., and Stipa, T.: A modelling system for the exhaust emissions of marine traffic and its application in the Baltic Sea area, Atmos. Chem. Phys., 9, 9209–9223, doi:10.5194/acp-9-9209-2009, 2009.

Kasper, A., Aufdenblatten, S., Forss, A., and Burtscher, H.: Particulate emissions from a low-speed marine diesel engine, Aerosol Sci. Tech., 41, 24–32,

doi:10.1080/02786820601055392, 2007.
Lack, D. A., Corbett, J. J., Onasch, T., Lerner, B., Massoli, P., Quinn, P. K., Bates, T. S., Covert, D. S., Coffman, D., Sierau, B., Herndon, S., Allan, J., Baynard, T., Lovejoy, E., Ravishankara, A. R., and Williams, E.: Particulate emissions from commercial shipping: Chemical, physical, and optical properties, J. Geophys. Res., 114, D00F04, doi:10.1029/2008JD011300, 2009.
Man Diesel and Turbo: MAN B&W 6S90ME-C7 Project guide, electronically controlled two-stroked engines, 5. edition, MAN Diesel, Teglholmsgade 41, DK-2450 Copenhagen, Denmark, 2009.
Matthias, V., Bewersdorff, I., Aulinger, A., and Quante, M.: The Contribution of Ship Emissions to Air Pollution in the North Sea Regions, Environ. Pollut., 158, 2241–2250, doi:10.1016/j.envpol.2010.02.013, 2010.
Matulja, D. and Dejhalla, R.: A Comparison of a ship hull resistance determined by different methods, Eng. Rev., 27(2), 13–24, 2007.
Moldanová, J., Fridell, E., Popovicheva, O., Demirdjian, B., Tishkova, V., Faccinetto, A., and Focsa, C.: Characterisation of particulate matter and gaseous emissions from a large ship diesel engine, Atmos. Environ., 43, 2632–2641, doi:10.1016/j.atmosenv.2009.02.008, 2009.
Murphy, S. M., Agrawal, H., Sorooshian, A., Padro, L. T., Gates, H., Hersey, S., Welch, W. A., Jung, H., Miller, J. W., Cocker III, D. R., Nenes, A., Jonsson, H. H., Flagan, R. C., and Seinfeld, J. H.: Comprehensive simulataneous shipboard and airborne characterization of exhaust from a modern container ship at sea, Environ. Sci. Technol., 43, 4626–4640, doi:10.1021/es802413j, 2009.
Paxian, A., Eyring, V., Beer, W., Sausen, R., and Wright, C.: Present-Day and Future Global Bottom-Up Ship Emission Inventories Including Polar Routes, Environ. Sci. Technol., 44, 1333–1339, doi:10.1021/es9022859, 2010.
Petzold, A., Hasselbach, J., Lauer, P., Baumann, R., Franke, K., Gurk, C., Schlager, H., and Weingartner, E.: Experimental studies on particle emissions from cruising ship, their characteristic properties, transformation and atmospheric lifetime in the marine boundary layer, Atmos. Chem. Phys., 8, 2387–2403, doi:10.5194/acp-8-2387-2008, 2008.
Petzold, A., Weingartner, E., Hasselbach, J., Lauer, P., Kurok, C., and Fleischer, F.: Physical properties, chemical composition and cloud forming potential of particulate emissions from a marine diesel engine at various load conditions, Environ. Sci. Technol., 44, 3800–3805, 2010.
Sarvi, A., Fogelholm, C.-J., and Zevenhoven, R.: Emissions from large-scale medium-speed

diesel engines: 1. Influence of engine operation mode and turbocharger, Fuel Proc. Tech., 89, 510–519, doi:10.1016/j.fuproc.2007.10.006, 2008a.
Sarvi, A., Fogelholm, C.-J., and Zevenhoven, R.: Emissions from large-scale medium-speed diesel engines: 2. Influence of fuel type and operating mode, Fuel Proc. Tech., 89, 520–527, doi:10.1016/j.fuproc.2007.10.005, 2008b.
Schrooten, L., De Vlieger, I., Panis L. I., Chiffi, C., and Pastori, E.: Emissions of maritime transport: A European reference system, Sci. Total Environ., 408, 318–323, doi:10.1016/j.scitotenv.2009.07.037, 2009.
Watson D. G. M.: Practical Ship Design, Elsevier, Oxford, UK, 76 pp., 1998a.
Watson, D. G. M.: Practical Ship Design, Elsevier, Oxford, UK, 219 pp., 1998.
Watson, Gilfillan, Somes hip design methods, Royal Institute of Naval Architects, 1976
Wild, Y.: Container Handbook, Vol 3, Refrigerated containers and CA technology, Gesamtverband der Deutschen Versicherungswirtschaft e.V., Berlin, 2009.
Winnes, H. and Fridell E.: Particle emissions from ships: Dependence on fuel type, J. Air Waste Manage. Assoc., 59, 1391–1398, doi:10.3155/1047-3289.59.12.1391, 2010a.
Winnes, H. and Fridell, E.: Emissions of NO_x and particles from Maneuvering Ships, Transportation Research D, 15, 204–2011, doi:10.1016/j.trd.2010.02.003, 2010b.

ACPD
11, 22129–22172, 2011

An assessment model of ship traffic exhaust emissions

J.-P. Jalkanen et al.

Table 1. Statistical measures for the power predictions of STEAM and STEAM2. P_M is the predicted power, is the measured power and the number of observations $n = 729$. Errors in percent in the table have been computed with respect to the mean values ofthe measurements.

	Formula	STEAM2	STEAM	Measured (M)
Mean value	$\frac{1}{n}\sum P$	11 190 kW	12 130 kW	12 338 kW
Mean Error	$\frac{1}{n}\sum(P - P_M)$	−1148 kW(−9.3 %)	−206 kW(−1.7 %)	–
Mean Absolute Error	$\frac{1}{n}\sum(\lvert P - P_M\rvert)$	1845 kW (15 %)	2267 kW (18.4 %)	–

ACPD
11, 22129–22172, 2011

An assessment model of ship traffic exhaust emissions

J.-P. Jalkanen et al.

Table A1. Fraction of draught values for different ship types to be used in estimation of propeller diameter unless it is specifically known or can be estimated with the methods described in the text.

Ship Type	Fraction of Draught	Ship Type	Fraction of draught
RoRo/Passenger	0.75	General Cargo	0.52
Cruise Ship	0.75	Icebreaker	0.5
RoRo Cargo	0.75	Other Ship	0.63
Bulk Cargo	0.46	Crude Oil Tanker	0.44
Container Cargo	0.62	LPG Tanker	0.53
Dredger	0.5	Oil Product Tanker	0.48
Chemical Tanker	0.5	Car Carrier	0.65
Fishing vessel	0.66	Tug, default	0.5

ACPD
11, 22129–22172, 2011

An assessment model of ship traffic exhaust emissions

J.-P. Jalkanen et al.

Table B1. Measured specific fuel-oil consumption values as a function of engine load, as reported in Wärtsilä (2007) for four-stroke engines. This set of data includes the measurements of "46" engine family, the reported power of which ranges from 5850 kW (engine code 6L46) to 18 480 kW (16V46).

Load, %	SFOC $g\,kWh^{-1}$, base=178, STEAM2	SFOC, $g\,kWh^{-1}$, Wartsila 46, 1155 kW/cylinder	Relative consumption
10	216		1.212
15	210		1.182
25	201	204	1.130
30	197	199	1.107
35	193		1.086
40	190	190	1.067
45	187		1.051
50	185	183	1.037
55	183		1.026
60	181	181	1.016
65	180		1.009
70	179		1.005
75	178	178	1.002
80	178	178	1.002
85	179	178	1.004
90	179		1.008
95	181		1.015
100	182	183	1.024

Table B2. Specific fuel-oil consumption measurements as a function of engine load, extracted from MAN product guide for two-stroke engines. Data for MAN 6S90ME-C7 engine (two-stroke with fixed pitch propeller and high efficiency turbocharger) were extracted from available product specifications. Relative SFOC-values (increase of SFOC in comparison to the minimum value given in product specifications) have been computed using the specified SFOC value for each engine.

MAN 6S80ME-C8.2 25 080 kW		MAN 6S80MC-C8.2 25 080 kW		MAN 6S90ME-C7 29 340 kW	
Load, %	Rel. SFOC	Load, %	Rel. SFOC	Load, %	Rel. SFOC
35	1.043	35	1.041	50	1.022
50	1.016	50	1.016	70	1
65	1	65	1.002	100	1.024
85	1.004	85	1	–	–
100	1.023	100	1.016	–	–

Discussion Paper | Discussion Paper | Discussion Paper | Discussion Paper |

ACPD

11, 22129–22172, 2011

An assessment model of ship traffic exhaust emissions

J.-P. Jalkanen et al.

Title Page
Abstract Introduction
Conclusions References
Tables Figures
◂◂ ▸▸
◂ ▸
Back Close
Full Screen / Esc

Printer-friendly Version

Interactive Discussion

Table B3. Specific fuel-oil consumption measurements as a function of engine load, extracted from CAT engine documentations for four-stroke engines. Relative SFOC-values have been computed using the specified SFOC value for each engine.

CAT 3516 1350 kW		CAT 3508-B 1425 kW		CAT 3516-C 2240 kW	
Load, %	Rel. SFOC	Load, %	Rel. SFOC	Load, %	Rel. SFOC
16.3	1.345	18.8	1.095	14.8	1.134
23.1	1.261	32.8	1.051	21.1	1.075
32.1	1.203	54.2	1.013	27.1	1.069
55.1	1.090	71.0	1.000	62.7	1.000
91.1	1.005	88.8	1.014	81.1	1.009
94.4	1.044	94.7	1.071	84.8	1.080

ACPD
11, 22129–22172, 2011

An assessment model of ship traffic exhaust emissions

J.-P. Jalkanen et al.

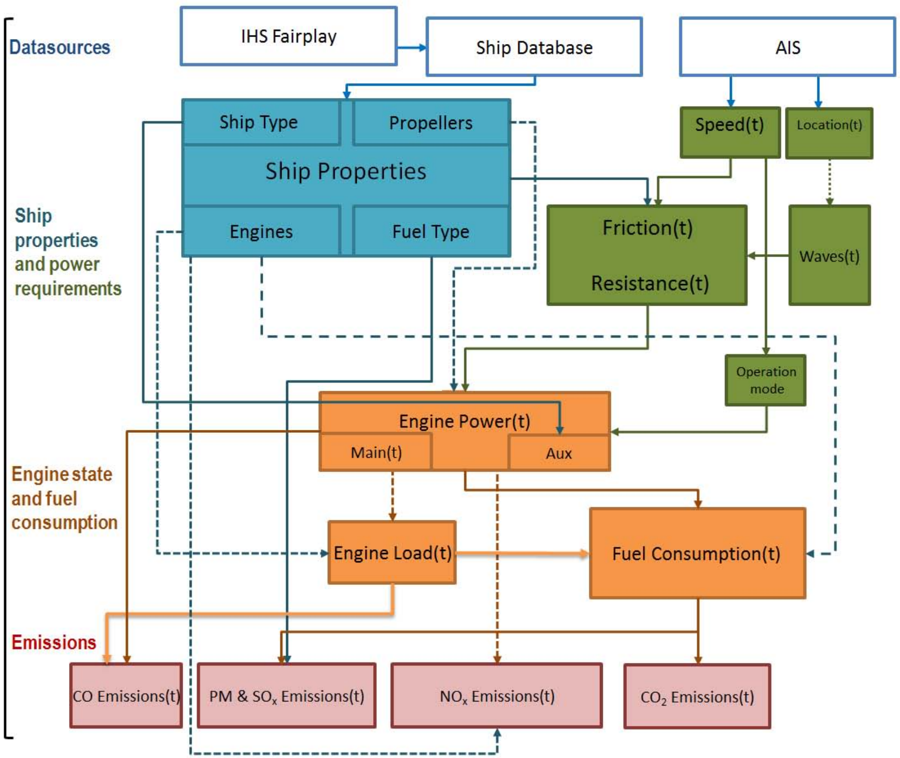

Fig. 1. A schematic diagram of the main components of the STEAM2 model and their interrelations. The model input data sources are presented on the uppermost row of rectangles, and the model output data (i.e. emissions) are presented on the lowest row of rectangles. The arrows describe either the flow of information in the model, or a modeled dependency between various factors. The different colors denote the various categories of factors included in the model; dotted and solid arrows are used only for visual clarity.

ACPD
11, 22129–22172, 2011

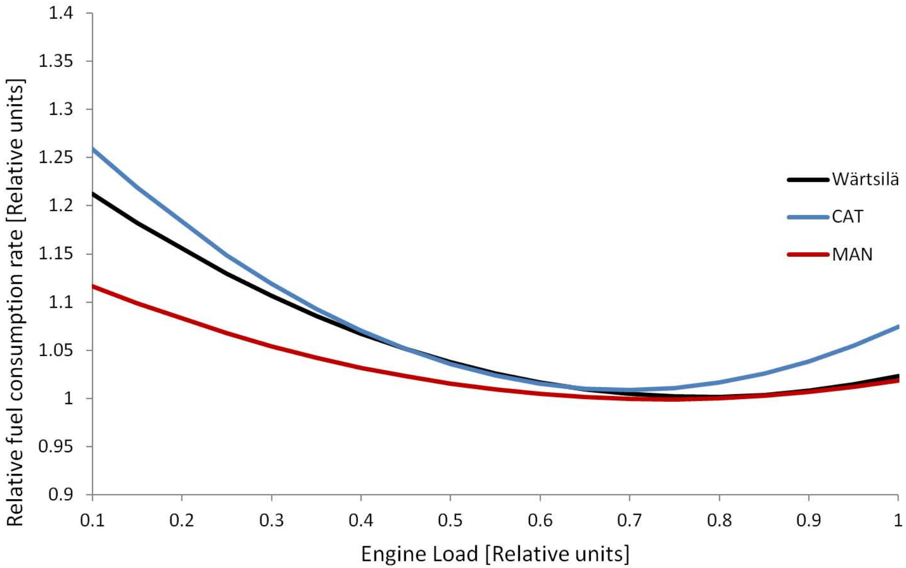

Fig. 2. The relative specific fuel-oil consumption (SFOC) as a function of the relative engine load, based on the data of three engine manufacturers: Wartsila, Caterpillar and MAN. The data of Caterpillar is based on three different SFOC-curves of small four-stroke engines (see Appendix B, Table B3), and the data of MAN is based on large two-stroke engines (see Appendix B, Table B2). Wartsila data for "46" engine family was used (see Appendix B, Table B1). A more detailed description of the data is presented in the main text and in Appendix B.

ACPD
11, 22129–22172, 2011

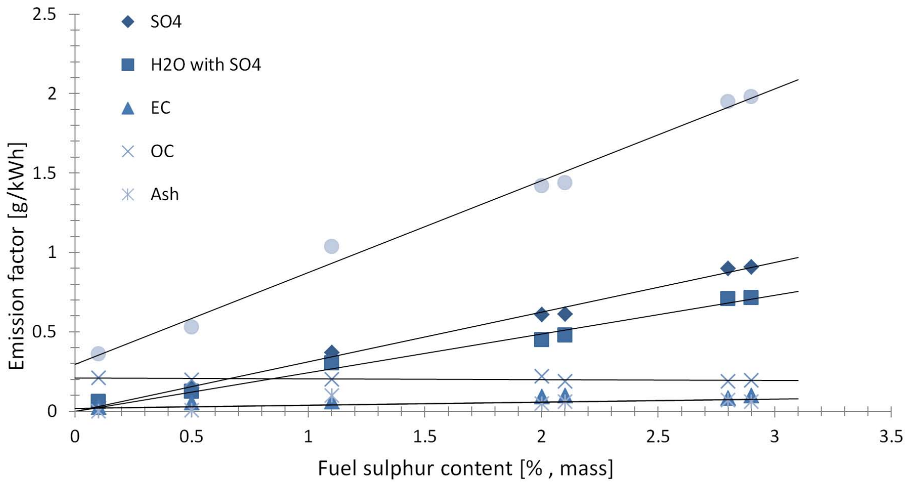

Fig. 3. The emission factor of the total PM, and for its chemical constituents as a function of fuel sulphur content (mass-based percentage), based on the data from the second IMO GHG study (Buhaug et al., 2009). Linear regression curves are presented as black lines. The emission factors of the total PM, SO_4 and H_2O are linearly dependent on the fuel sulphur content. The data points for EC and ash are partly overlapping in the figure.

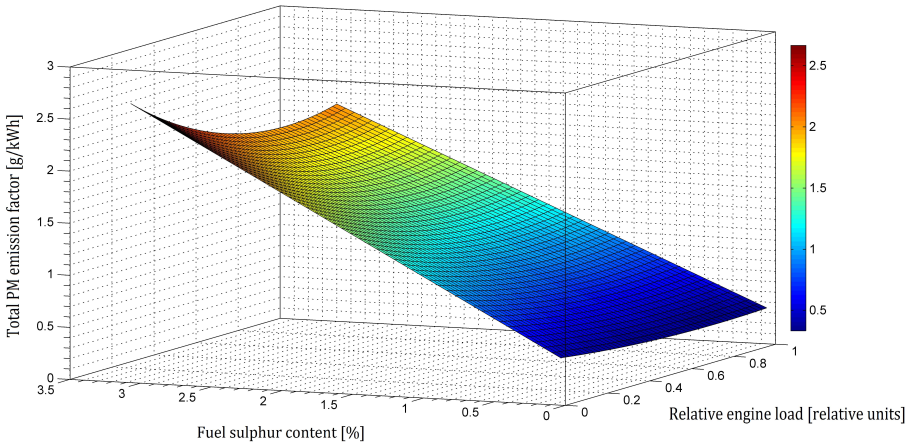

Fig. 4. The predictions of the STEAM2 model for total PM emission factor [legend, in units of $g\,kWh^{-1}$] as a function of engine load and fuel sulphur content.

ACPD
11, 22129–22172, 2011

Title Page
Abstract | Introduction
Conclusions | References
Tables | Figures
◄ | ►
◄ | ►
Back | Close
Full Screen / Esc
Printer-friendly Version
Interactive Discussion

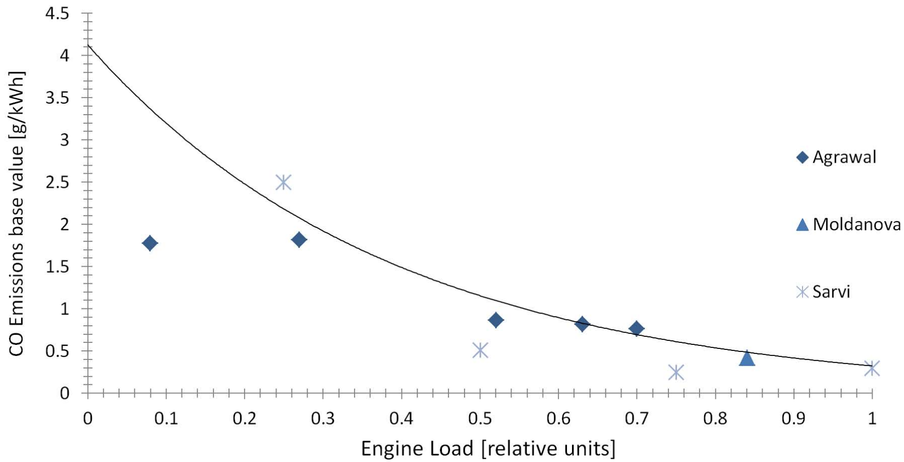

Fig. 5. The base valueof CO-emission as a function of relative engine load. The measurements of Agrawal, Moldanova and Sarvi have been shown, and the CO-base emission factor curve is based on Sarvi. The emissions of CO are also influenced by rapid changes of relative engine load.

ACPD
11, 22129–22172, 2011

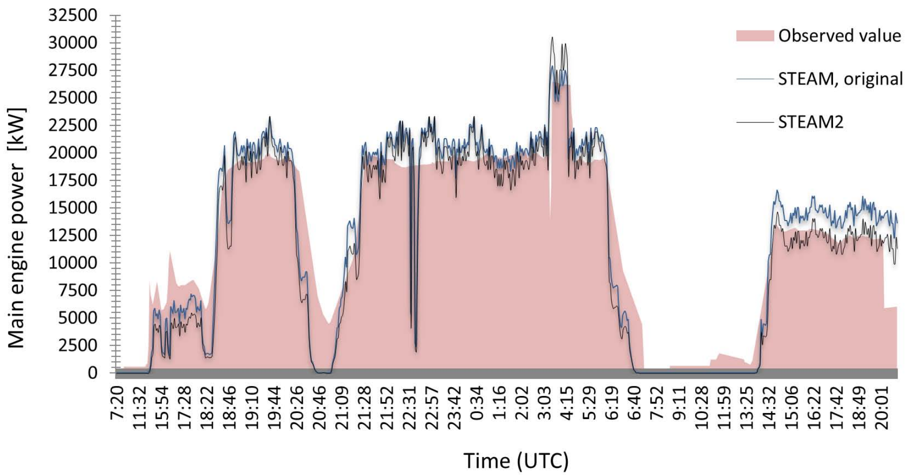

Fig. 6. The predictions of the STEAM and STEAM2 models and the corresponding measured engine power. The data has been measured for a 60 000t RoPax vessel that was sailing in the Baltic Sea within and near the archipelago surrounding the city of Stockholm in April 2008.

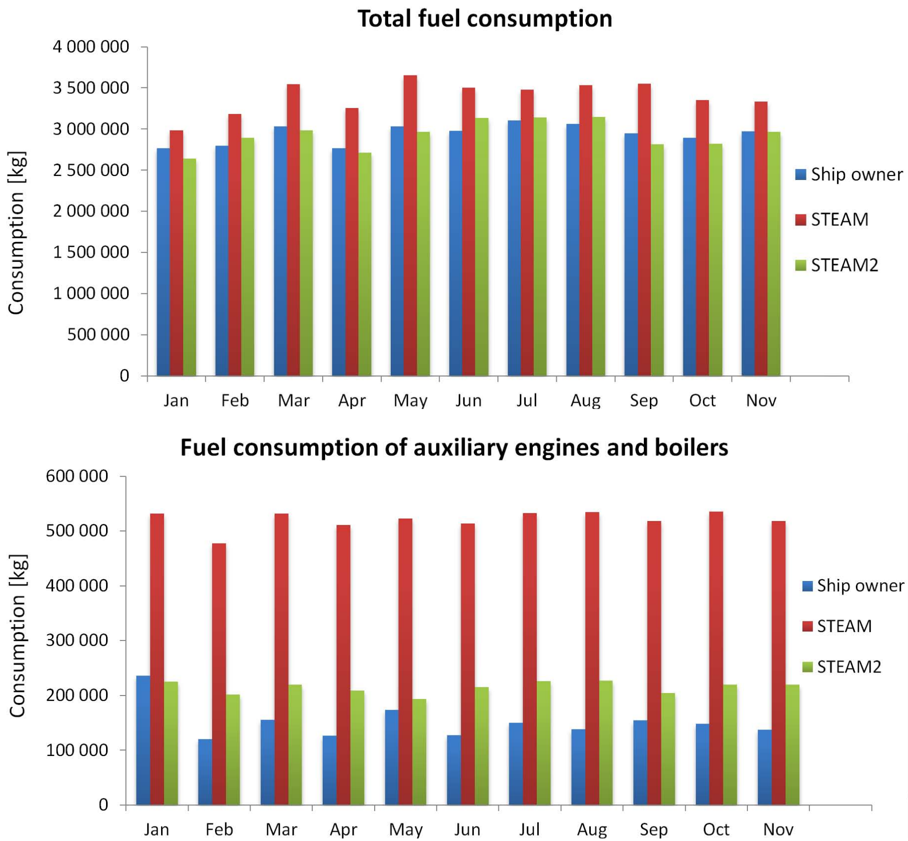

Fig. 7. The monthly average fuel consumption of a RoPax ship in 2007, as reported by the ship owner, and predicted by the two model versions. The total fuel consumption is presented in the upper panel, and the fuel consumption of auxiliary engines and boilers in the lower panel.

ACPD
11, 22129–22172, 2011

An assessment model of ship traffic exhaust emissions

J.-P. Jalkanen et al.

Title Page
Abstract | Introduction
Conclusions | References
Tables | Figures
◀| |▶
◀ ▶
Back | Close
Full Screen / Esc
Printer-friendly Version
Interactive Discussion

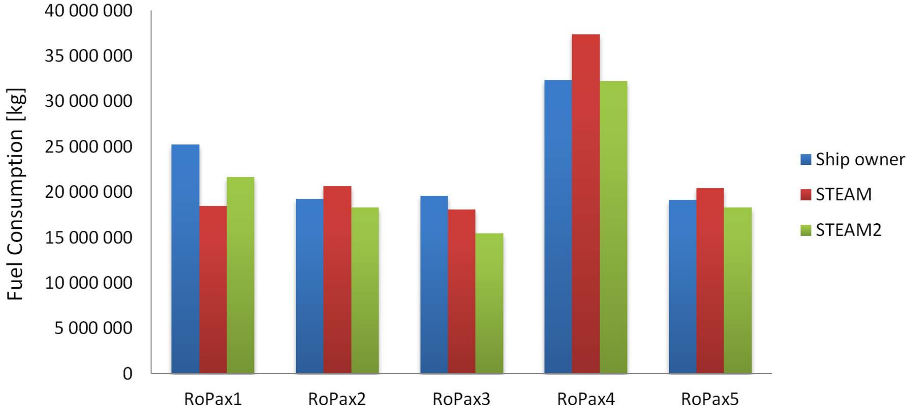

Fig. 8. The reported and predicted total fuel consumption for five RoPax vessels from January to November in 2007. The vessel RoPax 4 is the same ship, the data of which has been presented in Fig. 7a–b.

ACPD
11, 22129–22172, 2011

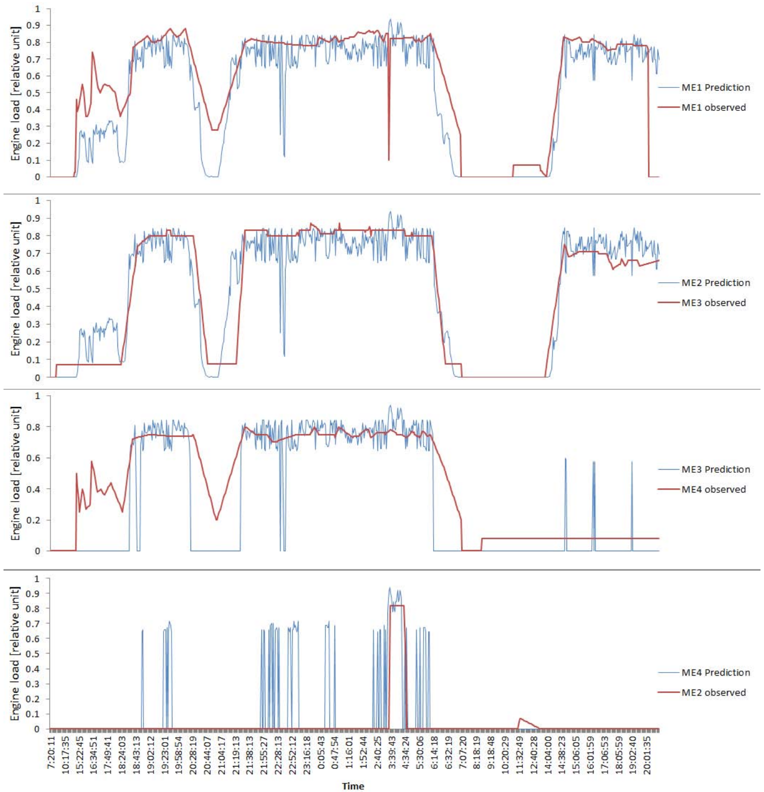

Fig. 9. Predicted and observed engine loads of four identical main engines in a large RoPax ship. The time scale for all plots **(a–d)** is the same, presented in **(d)**.MEx, $x = 1, 2, 3, 4$, are the four main engines. The numbering of the main engines in the model has no influence on the engine load predictions; for instance, in **(b)** the curves ME2 (estimate) and ME3 (observed) are directly comparable.

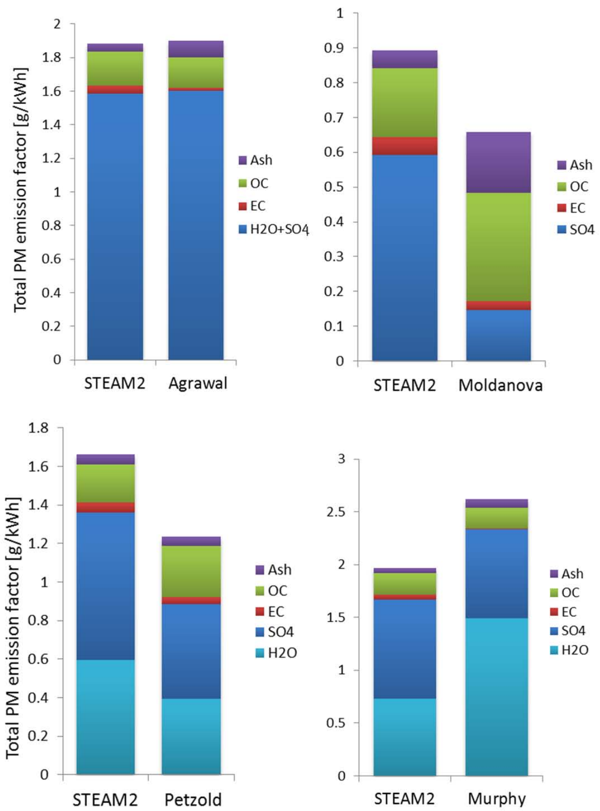

Fig. 10. Comparison of the predicted and measured emission factors for the chemical constituents of PM. The measured data has been extracted from Agrawal et al. (2008b), Moldanova et al. (2009), Petzold et al. (2008) and Murphy et al. (2009).

ACPD
11, 22129–22172, 2011

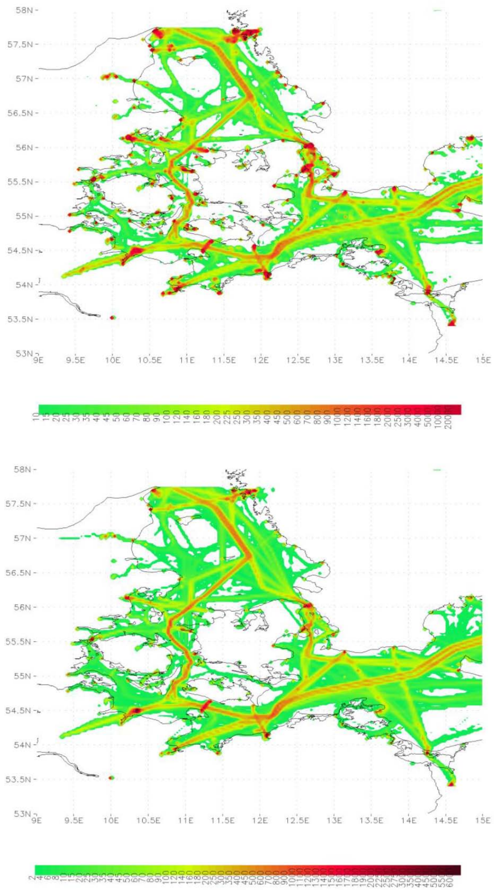

Fig. 11. Predicted geographical distribution of CO (upper panel) and PM emissions (lower panel) from shipping in the marine regions surrounding the Danish Straits in January 2009. The color scale corresponds to emissions in kilograms of CO or PM originated from grid of $1.9 \times 3.4\,km^2$ (0.03 degrees).

ACPD
11, 22129–22172, 2011